Materials Advances

ROYAL SOCIETY OF CHEMISTRY

PAPER

Check for updates

Uniformly distributed graphite with dual attributes to achieve enhanced mechanical and tribological properties of PEK-C/graphite composites *via* a precipitation method†

Zengwen Cao, [ID] Zhipeng Wang* and Guangyuang Zhou*

The agglomerative effect of graphite in polymeric materials is the main reason for the limited properties of such composites. In this work, amorphous cardo-polyetherketone (PEK-C) with excellent solubility was used to produce PEK-C/graphite composites *via* a precipitation method. The results illustrated that a uniform distribution of graphite was achieved in the PEK-C matrix, which completely displayed the dual properties of graphite. On the one hand, graphite was used as a filler to improve the mechanical properties of the material. On the other hand, graphite acted as a lubricant, which optimized the tribological properties. According to the time–temperature equivalence principle, at shorter test times, graphite hindered the initiation and propagation of cracks, which made the non-notched impact strength increase by 35.7%. At longer test times, graphite eliminated internal stress by facilitating segment motion, which prevented premature fracture and improved the tension toughness and strength of the composites. The morphologies of the dispersed phase were directly related to the viscoelastic properties of the composites, which allowed improvement of the lubrication and wear-resisting performance of the composites prepared *via* the precipitation method. This paper not only proposes a simple and facile technology to produce PEK-C/graphite composites, which could be used in industrial applications to save energy and reduce CO_2 emissions, but also emphasizes the importance of the state of the dispersed phase distribution. It is a typical example for understanding the relationship between structures and properties.

1. Introduction

In recent years, with more and more attention being paid to energy consumption and environmental pollution, high-performance tribological materials with excellent mechanical properties are required to conserve energy and reduce carbon dioxide emissions. Up to now, it remains a challenge to prepare high-performance tribological materials with excellent tribological properties, dimensional stability and aging-resistance in high load-bearing and sliding-velocity environments. Among the many available materials, poly(aryletherketone) (PAEK) is a characteristic thermo-plastic polymer material with prominent mechanical properties, thermal stability and self-lubricating properties, which makes it a typical engineering plastic for developing tribological composites. In addition, the cost of PAEK is lower than those of other special engineering plastics,

such as polyimide, polyetherimide and so on. These characteristics make PAEK a vital matrix for preparing high-performance polymer-based tribological materials. However, both the high frictional coefficient at low sliding velocity and the frictional vibration phenomenon tremendously restrict the utilization of PAEK friction materials. A lot of efforts have been made to improve the tribological properties of PAEK *via* the addition of lubricants like polytetrafluoroethylene, carbon fiber, glass fiber, carbon nanotubes, graphite and so on.[1–9] Among these, graphite has a low friction coefficient, low density, excellent thermal conductivity, high temperature resistance and good chemical stability, and thus has attracted major attention as a valid lubricating agent.

The tribological and mechanical properties of composites are influenced by their phase structure, including filler size, amount, shape and distribution, and the interface strength between the matrix resin and filler.[10–15] Lu *et al.* illustrated that the frictional coefficient and wear rate of PEEK were obviously decreased when graphite was added.[6] The relationship between graphite size and the performance of composites with graphite has been investigated by Shang and Zhao *et al.*[3] They reported

that both the anti-wear and mechanical properties of PEEK/graphite composites were enhanced as the particle size decreased from 150 to 10 μm. Nevertheless, the optimal size and content of graphite is closely related with the graphite distribution. Currently, there is still a lack of an efficient and convenient method to produce such composites with uniformly distributed graphite particles. Graphite has strong van der Waals forces, a large specific surface area and poor interfacial compatibility with polymer matrices. It is easy to produce graphite agglomerations by direct melt-mixing with PAEK. Furthermore, the melt-blending temperature of PAEK is very high, usually more than 300 °C, which requires better equipment and higher energy consumption. By comparison, solution-processible techniques are popular methods to produce uniformly distributed polymer matrix composites.[16] Despite this, solution processing has been rarely applied to PAEK due to its chemical inertness (it is almost insoluble in any solvent).[17]

Cardo-polyetherketone (PEK-C), as an important member of the polyaryletherketone (PAEK) family, has outstanding thermal stability, mechanical behaviors, corrosion resistance, irradiation stability, hydrolytic resistance and self-lubricating properties. More importantly, the non-planar cardo groups on the PEK-C main chains reduce the regularity of chain segments and the crystallization performance, which means that amorphous PEK-C dissolves well in some organic solvents, such as dimethylacetamide, *N*-methyl pyrrolidone, *N*,*N*-dimethylformamide and so on. The cardo groups not only make solution processing possible for PEK-C/graphite systems, but also provide graphite with more free volume in which to distribute and dipole–dipole interaction force sites to adhere with the polymer.

So, in this work, taking advantage of the solubility of PEK-C, we provide a simple and effective route to prepare PEK-C/graphite composites with excellent tribological and mechanical properties *via* a precipitation approach. PEK-C was chosen as the polymer matrix since it has good solubility in *N*,*N*-dimethylacetamide (DMAc). Both mechanical blending and solution mixing were used to manufacture PEK-C/graphite composites for exploring the influence of the processing method on the phase distribution. The relationship between the dispersiveness of graphite and the mechanical and frictional performance was carefully investigated. The lubrication and wear-resistance mechanism of PEK-C/graphite was proposed with the help of scanning electron microscopy, thermal conductivity testing, rotational rheometry and so on.

2. Experimental

2.1. Materials

PEK-C with a reduced viscosity of 0.57 dL g^{-1} was provided by Zhejiang Paek New Materials Co., Ltd. (China) under the trade name PEKC-01. Fig. 1 displays the structural formula of the polymer. The size of the graphite was less than 45 μm, and it was obtained from Nanjing Jiaoziteng Scientific Equipment Co., Ltd. (China). *N*,*N*-Dimethylacetamide was offered by
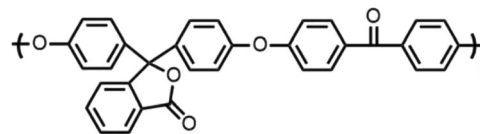

Fig. 1 The structural formula of PEK-C.

Guangdong Guanghua Sci-Tech Co., Ltd. Anhydrous alcohol of analytical grade was purchased from Tianjin Fuyu Fine Chemical Co., Ltd.

2.2. Preparation of PEK-C/graphite composites

30 wt% graphite was chosen to explore the effect of the preparation process on the structure and properties of PEK-C composites after preliminary experiments, as shown in Fig. S1 and S2 (ESI†). The high-performance composite powders of PEK-C/graphite were obtained *via* precipitation methodology. Firstly, PEK-C was dissolved in *N*,*N*-dimethylacetamide solvent at 5 wt%. In order to accelerate the dissolution of PEK-C, the temperature and stirring rate of the solution were set at 80 °C and 230 rpm, respectively. After PEK-C was completely dissolved, 30 wt% graphite was added into the PEK-C solution and the mixture was stirred steadily for another 30 min. Then, *N*,*N*-dimethylacetamide was continuously evaporated at 190 °C until the concentration of PEK-C reached 15 wt%, immediately followed by cooling the temperature of the suspension to 90 °C. The final suspension was slowly poured into a precipitant containing 66.67 wt% anhydrous alcohol and 33.33% deionized water. Subsequently, the strip-shaped sediments were pulverized and washed with boiling water to remove residual *N*,*N*-dimethylacetamide solvent. Lastly, the composite powder of PEK-C/graphite was dried in a drum wind drying oven at 150 °C for 24 h. As a comparison, a PEK-C matrix composite powder with 30 wt% graphite was also produced *via* mechanical blending using a high-energy ball-milling machine. The procedure was set as 350 rpm for 1 h and then 550 rpm for 4 h.

These PEK-C/graphite powders were compression-molded into composite plates with different external dimensions. The moulding temperature, and pressure and time of compression molding were set as 320 °C, 8 MPa and 40 min, respectively. According to testing standards, the composite plates were cut into test bars of various sizes using a numerical control engraving machine (Jingyan Instrument Technology Co., Ltd). The composites produced using different processing methods were designated as CZ-X, as listed in Table 1.

2.3. Characterization

2.3.1. Morphology characterization. Cryofractured and worn surface images of the PEK-C/graphite composites were obtained *via* a field emission scanning electronic microscope (KYKY, EM6900, China), operated at 20 KV. The directly heated cathode of the scanning electron microscope was tungsten. In order to clearly observe the morphological features of the composites, the beam and electronic current were set as 120 μA and 2.5 Å, respectively. All surfaces were coated with gold at 7 mA for 50 s.

Table 1 The differences between designated samples

	PEK-C content (wt%)	Graphite content (wt%)	Blending method	Molding method
CZ-3	70	30	Mechanical blending	Hot compacting
CZ-5	70	30	Solution blending	Hot compacting

2.3.2. Thermal properties. Differential scanning calorimetry (DSC) measurements were carried out to estimate the influence of graphite on the thermal properties of the PEK-C matrix, using differential scanning calorimetry equipment (TA Instruments DSC 25, USA). Specimens with a weight between 5 and 10 mg were sealed into aluminum pans. A three-scan characterization procedure was implemented with a 0.1 MPa nitrogen press: (1) a first heating process from 30 °C to 380 °C at a rate of 10 °C min^{-1}, maintaining the temperature for 3 minutes to remove the thermal history; (2) cooling from 380 °C to 30 °C at a rate of 40 °C min^{-1}; (3) a second heating process from 30 °C to 380 °C at a rate of 10 °C min^{-1} to determine the glass transition temperature (T_g).

The rheological properties of the PEK-C/graphite composites, including the storage modulus, loss modulus and complex viscosity, were measured using a hybrid rheometer (Discovery HR-2, USA). The tests were conducted in frequency sweeping mode at 320 °C. The shear frequency was set between 100 and 0.1 rad s^{-1} with an invariable strain of 1.25%. Before experiments, the samples were transferred into a parallel plate–plate configuration with a diameter of 25 mm and equilibrated for 180 s.

2.3.3. Mechanical properties. According to the GB/T 1040-2006 standard, the experiments on tensile performances were conducted using a tensile testing machine (Instron 5566, USA). The elongation rate was set as 1 mm min^{-1}. The notched and non-notched Izod impact strength of the PEK-C/graphite composites was assessed following GB/T 1843-2008. Rectangular specimens with a size of 80 × 10 × 35 mm were tested in dual-cantilever mode. All measurements were repeated five times and the average value calculated to eliminate error.

2.3.4. Tribological properties. The frictional coefficient and anti-wear rate of the PEK-C/graphite composites were evaluated employing an HRB-3F ring–block friction and wear testing machine (Jinan HengXu Testing Machine Technology Co., Ltd, China) referring to GB/T 12444-2006. Before the friction testing, the surfaces of the samples were polished using an engraving machine (CNC4030, JingYan Instruments and Technology Co., Ltd, China). These test blocks were fixed on a clamp against an annular friction pair. The normal load and sliding velocity were adjusted to determine the tribological performances under different application environments. The normal load refers to the force perpendicular to the friction surface between the sample and the friction pair, and was set as 66 N during the test. The effect of the normal load on the tribological properties of the composites had been investigated, as per the results shown in Tables S3 and S4 and Fig. S3 and S4 (ESI†). The A value (mass wear rate) was calculated according to eqn (1):

$$A = (m_1 - m_2)/(m_1) \times 100\% \tag{1}$$

where m_1 refers to the pre-test quality of the test block and m_2 is the post-test quality of the test block.

3. Results and discussion

PAEK is a characteristic thermo-plastic polymer material with prominent mechanical properties, thermal stability and self-lubricating properties, which make it typical engineering plastic for developing tribological composites. However, it is difficult to control the dispersion and morphology of the filler in the polymer matrix. Even if the composites have the same composition, different processing technologies induce various
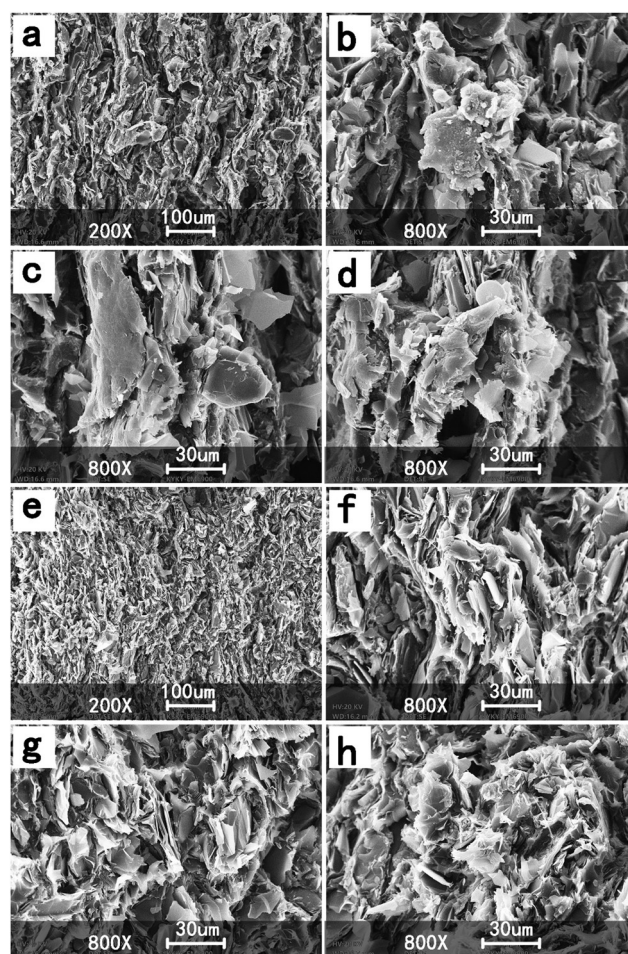

Fig. 2 SEM micrographs of the cryogenic fracture surfaces of the composites: (a) 200× magnified image of CZ-3; (b)–(d) 800× magnified images of CZ-3; (e) 200× magnified image of CZ-5; (f)–(h) 800× magnified images of CZ-5.

phase structures. Consequently, the structure–property relationship of the PEK-C/graphite composites will be further discussed based on the precipitation method, which was a new processing technology for PAEK and was realized as a result of the non-planar cardo groups of PEK-C.

3.1. Morphological features of PEK-C/graphite composites

The properties of the PEK-C/graphite composites were related to their phase morphologies. SEM was employed to characterize the morphological features of the composites prepared *via* different processing technologies, and the micrographs of the cryogenic surfaces are displayed in Fig. 2. For the SEM image under a visual field at 200×, the transverse surface of CZ-3 was covered with large rough and uneven gullies. It was easy to find obvious large banded structures randomly distributed in the composite. These fluctuating aggregates could be observed more clearly under a field of view at 800×, suggesting poor dispersibility of graphite leading to serious separation of the dispersed phase and matrix phase. In contrast to CZ-3, CZ-5 fabricated through the precipitation approach showed a more uniform and delicate frozen section in the 200× SEM pictures, which indicated that the dispersibility of graphite in the PEK-C matrix was enormously promoted. After solution blending, the sizes and gaps of gullies clearly lessened and homogenized in the composite. In the 800× microscopic images, the PEK-C/graphite cross-sections presented a homogeneous and distinct lamellar structure. The disappearance of large banded structures confirmed that the precipitation made the graphite more homogeneous in the PEK-C matrix than it was in CZ-3.

3.2. Thermal properties of PEK-C/graphite composites

The thermal properties, such as glass-transition temperature (T_g), storage modulus, loss modulus and complex viscosity were affected by the dispersion between the graphite and PEK-C matrix. The DSC profiles of the composites are presented in Fig. 3. The T_g of CZ-3 in the first-heating profile was lower than that of CZ-5, which meant that the inhibiting effect of graphite on the polymer matrix was weaker in the former. This was in accordance with the inferior dispersibility of graphite in CZ-3. The specific data are summarized in Table 2. In addition to

Table 2 The thermal performances of the PEK-C/graphite composites (T_{g1} means the T_g in the first heating run; T_{g2} means the T_g in the second heating run)

	T_{g1} (°C)	T_{g2} (°C)	T_{g2}–T_{g1} (°C)
CZ-3	227.1	229.8	2.7
CZ-5	228.3	228.2	−0.1

this, the T_g in the second-heating profile was 2.7 °C higher than the T_g in the first-heating profile for CZ-3, which was attributed to re-dispersion of graphite during the first-heating and equilibrating processes. It was interesting to find that the T_g of CZ-5 was about same in the first- and second-heating curves. The similar values illustrated that the dispersion state of graphite after solution mixing was uniform.

In general, the graphite played two roles in the composites. On the one hand, graphite, as a filler, hindered the chain mobility, which was proved by DSC experiments. On the other hand, graphite acted as a lubricant to accelerate the chain motion of the polymer, especially in the presence of external forces. The melt rheological property measurements of the PEK-C/graphite composites reflected the changes in state of the polymer chains in response to shear force. As shown in Fig. 4, CZ-5 exhibited a lower storage modulus, loss modulus and complex viscosity than CZ-3. Taking complex viscosity as a typical example, a lower shear viscosity of the composite implied better lubrication effects exerted by graphite, which was related to superior dispersibility of the filler. In the precipitation process, the chains of the polymer gradually wrapped the graphite particles with the help of the solvent. Therefore, the uniformity of the dispersed phase was better in CZ-5 than in CZ-3, as demonstrated earlier, which led to a lower complex viscosity. In contrast with the storage modulus, loss modulus and complex viscosity, the loss angle tangent (tan δ) of CZ-5 was higher than that of CZ-3, which corresponded to more energy dissipation in CZ-5 during the process of measurement. Meanwhile, the larger tan δ meant that the polymer matrix of the composite tended to be viscous rather than elastic, although both polymers were viscoelastic. The findings are also attributed to the well-distributed graphite in CZ-5, which promoted disentanglement and irreversible flow of polymer
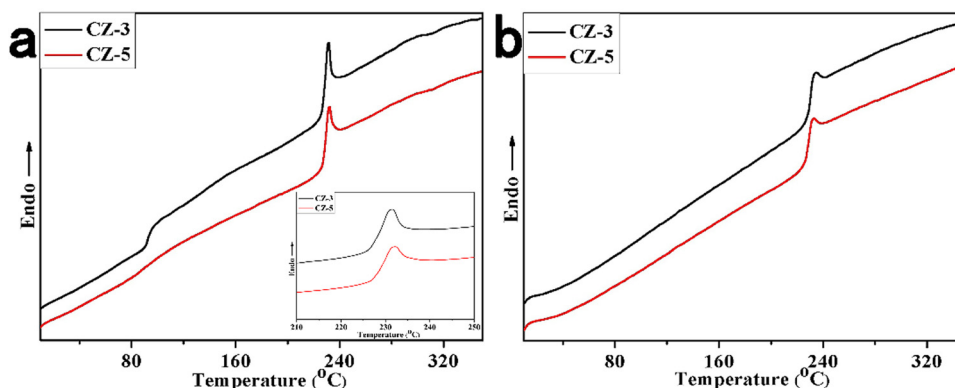

Fig. 3 The heating thermograms of the PEK-C/graphite composites: (a) the first-heating curves; (b) the second-heating curves.
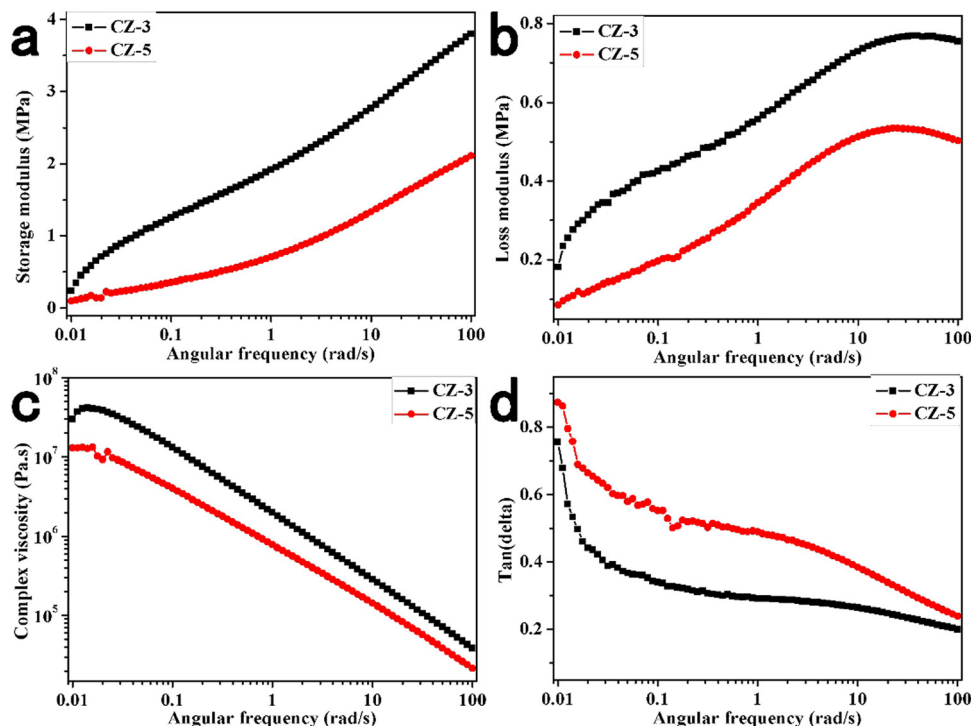
Fig. 4 The melt rheological properties of the PEK-C/graphite composites: (a)–(d) the evolution of the storage modulus (G'), loss modulus (G''), complex viscosity ($|\eta^*|$) and loss angle tangent ($\tan\delta$) *versus* angular frequency at 320 °C, respectively.

chains. So, the results were consistent with the storage modulus, loss modulus and complex viscosity.

3.3. Mechanical properties of PEK-C/graphite composites

The mechanical performance, including tensile properties and impact strength, was characterized *via* tensile and impact tests, respectively. As shown in Table 3, CZ-5 had higher tensile strength, elongation at break, notched impact strength and non-notched impact strength than CZ-3, which indicated that the composite prepared *via* precipitation method displayed toughening and strengthening at the same time. As displayed in Fig. 5, PEK-C and its composites did not yield, with typical hard and brittle material characteristics. With the increase in tensile strain, the tensile stress increased gradually until the material broke. Among the materials, CZ-5 showed comprehensive properties of higher toughness and strength. The basic reason for the toughening and strengthening was that the uniformly dispersed graphite had a dual nature, *i.e.*, as a filler limiting segmental motion and as a lubricant promoting
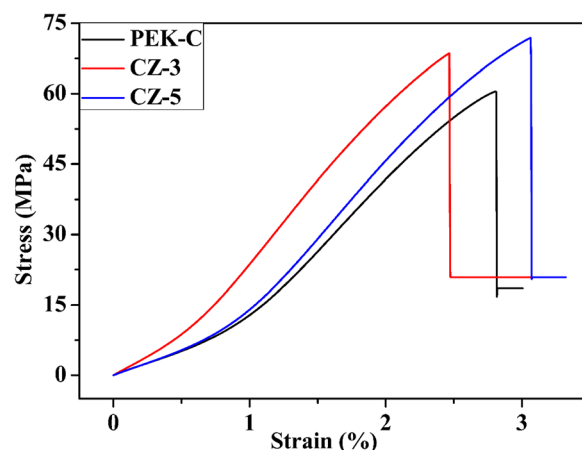

Fig. 5 The typical stress–strain curves of the PEK-C/graphite composites.

segment motion. In the initial stretching stage, the well-dispersed graphite eliminated internal stress by facilitating segment motion, which prevented premature fracture and improved the elongation at break of the composite. In the late period of the tensile measurements, homogeneously dispersed graphite obstructed crack development and so increased the tensile strength. The higher impact strength of CZ-5 than that of CZ-3 was also ascribed to the phase distribution state. The more uniform distribution of the matrix and filler meant that cracks were more difficult to initiate and propagate. Combined with the SEM imaging observations, it was obvious that the

Table 3 Mechanical properties of the PEK-C/graphite composites

Mechanical properties	PEK-C	CZ-3	CZ-5
Tensile modulus (GPa)	3.14	3.67	3.38
Tensile strength (MPa)	60.28	63.76	70.86
Elongation at break (%)	2.65	2.37	3.05
Notched impact strength (KJ m^{-2})	6.05	5.93	6.07
Non-notched impact strength (KJ m^{-2})	8.91	9.41	12.77

Table 4 The tribological properties of PEK–C/graphite composites

	Pre-test quality (g)	Post-test quality (g)	Wear scar width (mm)	Mass wear rate (%)
CZ-3-water	2.373	2.370	2.0	0.126
CZ-3-dry	2.368	2.363	4.0	0.211
CZ-5-water	2.021	2.020	3.0	0.099
CZ-5-dry	2.024	2.024	2.0	0.000

sizes and gaps of the gullies were clearly lessened and more homogenized in CZ-5 than in CZ-3, which made the notched impact strength and non-notched impact strength increase by 2.4% and 35.7%, respectively.

3.4. Tribological properties of PEK–C/graphite composites

The frictional properties of the PEK–C/graphite composites were evaluated *via* their friction coefficient and abrasion rate, which are shown in Table 4. It could be seen that the frictional coefficient of CZ-5 was lower than that of CZ-3 in water when the linear velocity was less than or equal to 0.74 m s^{-1} (Fig. 6a). If the linear velocity in the experiments exceeded 0.90 m s^{-1}, the water friction coefficient of CZ-5 became higher than that of CZ-3. Broadly speaking, the difference between the water friction coefficient values of CZ-5 and CZ-3 was small, which was attributed to water replacing the PEK–C/graphite composites as a lubricant. In the dry friction experiment environment, the morphological, thermal and mechanical characteristics of the composites directly influenced the tribological properties. As shown in Fig. 6b, the coefficient of dry friction was lower for CZ-5 than for CZ-3 within the linear velocity range of 0.045 to 2.24 m s^{-1}, which was due to the variation of viscoelasticity.

With an increase in temperature, the polymer could exhibit glassy, highly elastic and viscous states in turn. At low speed, frictional heat build-up was limited, which cause vitrescence of both CZ-3 and CZ-5. The better the tension toughness, the smaller the frictional resistance formed at the interface. When the linear velocity increased, the incremental frictional heat allowed the composite at the boundary to melt. Low complex viscosity was beneficial to decreasing the friction coefficient. Once the melt had transferred to the friction pair and then formed a transfer film by cooling, the higher tensile strength
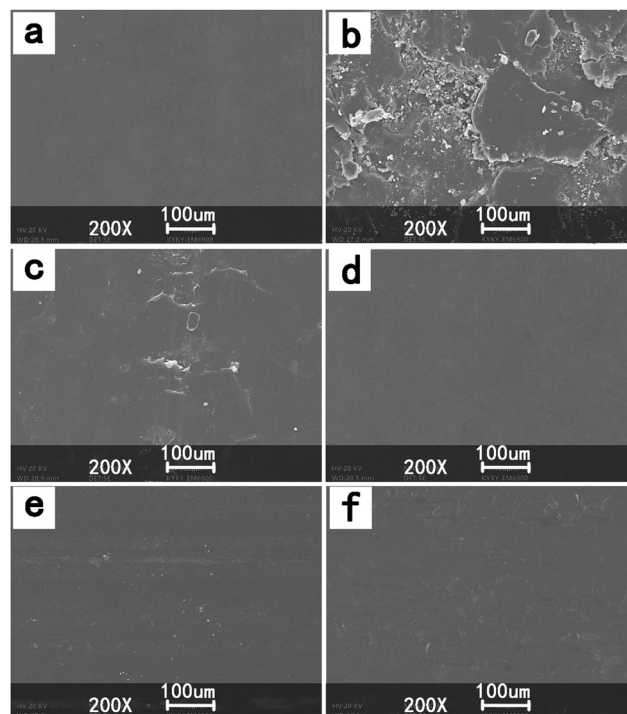

Fig. 7 SEM micrographs of worn surfaces of the PEK–C/graphite composites: (a) the surface of CZ-3 before friction testing; (b) the friction surface of CZ-3 after dry sliding; (c) the friction surface of CZ-3 after water lubrication; (d) the surface of CZ-5 before friction testing; (e) the friction surface of CZ-5 after dry sliding; (f) the friction surface of CZ-5 after water lubrication.

and impact strength of the composite ensured the integrity of the transfer film. The viscoelastic properties of the composites prepared *via* different blending methods were closely related to their phase structures, which were characterized *via* SEM. CZ-5 with a homogeneous phase structure could fully display the dual properties of graphite, which decreased the complex viscosity and improved the tensile and tension strength. Fig. 7 displays the worn-surface micrographs of the PEK–C/graphite composites. The surfaces of CZ-3 were significantly destroyed with well-defined pitted abrasive and fatigue wear observed *via* SEM. A large amount of wear debris aggregated on the worn surfaces of the composite, particularly on the surface
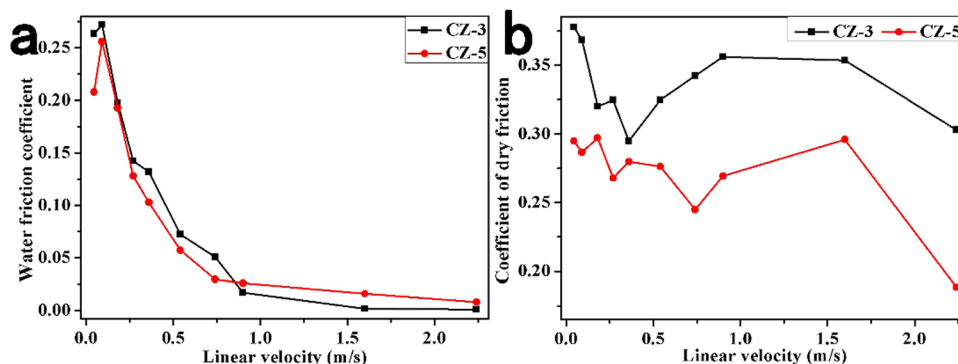

Fig. 6 The tribological properties of the PEK–C/graphite composites: (a) water friction coefficient; (b) coefficient of dry friction.
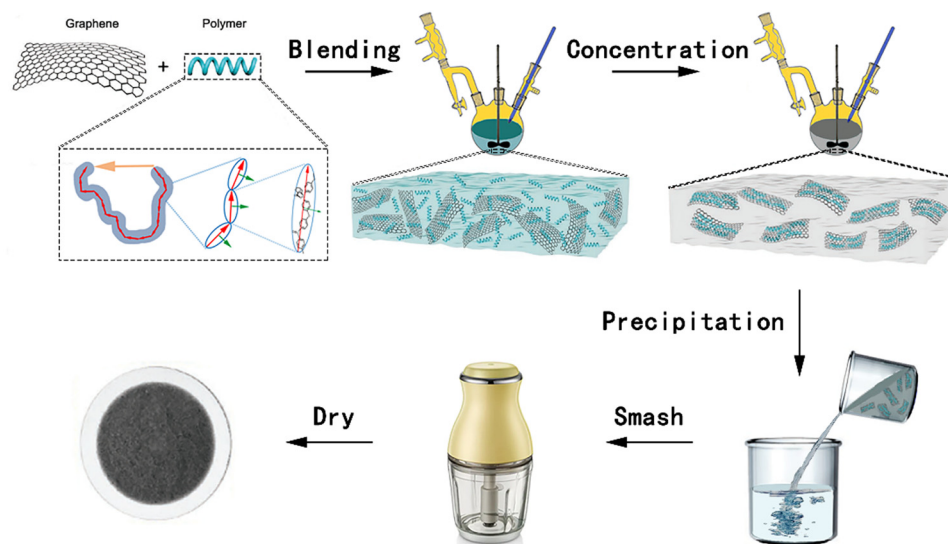
Fig. 8 The schematic diagram for the preparation of PEK-C/graphite composites by solution blending.

subjected to dry friction, which indicated that the heterogeneous graphite was peeled off from the PEK-C/graphite composite. Both in dry and water frictional environments, the worn surfaces of CZ-5 were smooth with little damage, which was closely related to the uniformly distributed graphite phase. The results further supported the thesis about the differences in tribological properties of CZ-3 and CZ-5 composites. So, the PEK-C/graphite composite produced *via* precipitation technology had better tribological properties.

3.5. Mechanism and value of precipitation method of composites

A uniform distribution of graphite in the PEK-C composite was realized by dilute solution blending, vaporizing the solvent and co-precipitation, just as displayed in Fig. 8. Although the individual polymer coils in the semidilute solution ($\sim$5%) overlapped and formed contacts with each other, the distribution of polymer structural units was uneven as a result of the extremely low concentration, which meant that the conformation of the molecular chains had a large non-Gaussian range and non-Gaussian characteristics. As the concentration gently increased, the degree of molecular chain aggregation, penetration and overlapping was enhanced. In this process, graphite was gradually and tightly wrapped with the polymer coils. The boundary between concentrated and highly concentrated solution was called the "full Gaussian concentration", which was higher than 10 wt%.[18] When the concentration of the PEK-C solution reached the highly concentrated solution range (15 wt%) during the solvent evaporation process, the macromolecular chains in the solution fully overlapped and entangled, which made the distribution of each chain segment roughly uniform, forming a three-dimensional entangled network filled with solution and graphite. With the aggregation and entanglement occurring between macromolecular chains during solvent evaporation, the probability of graphite

aggregation formation decreased substantially, which has been proved by the SEM micrographs in Fig. 2.

Once the graphite was uniformly distributed in the PEK-C matrix, the thermal, mechanical and tribological performances of the composite would be greatly improved. Firstly, the evenly distributed graphite alleviated the stress concentration effect in the composite, which led to the avoidance of premature fracture due to high local stress and improved the strength of the composite material. Secondly, graphite was more fully wrapped with polymer molecular chains *via* the precipitation method. In all melt rheology tests, tensile property experiments and tribological characterizations, segmental motion of the polymer matrix was restrained by the lamellar graphite filler, which directly led to higher strength and wear resistance. Thirdly, the evenly distributed graphite continuously, uniformly and in an orderly way, migrated to the friction surface to reduce the frictional coefficient and wear rate of the composite along with the friction process. Thus, the distribution of graphite in PEK-C had a great influence on the properties of the composites, and could be adjusted *via* a simple solution blending and precipitation method.

4. Conclusion

Uniform dispersibility of graphite in PEK-C was achieved through a precipitation method. Using this technology, the dual properties of graphite were completely displayed. On the one hand, graphite as a filler enhanced the notched and non-notched impact strength of the composite. On the other hand, graphite as a lubricant promoted segment motion of the PEK-C matrix. Evenly distributed graphite promoted disentanglement and irreversible flow of polymer chains, which reduced the storage modulus, loss modulus and complex viscosity, and increased the loss angle tangent value. By regulating the mechanical and viscoelastic properties of the composites, the

composite prepared using precipitation has a lower friction coefficient and abrasion rate, especially under dry friction conditions. The coefficient of water friction and dry friction reached 0.008 and 0.1885, respectively. The biggest drop occurred at 37.78% when the linear velocity of dry friction was 2.24 m s^{-1}.

In brief, the graphite was homogeneously dispersed in the PEK-C substrate *via* the solution blending and precipitation method, which allowed the mechanical and tribological properties of the composite to be optimized. Thus, the study displayed an excellent strategy to regulate the morphologies of composites and produce high-performance composites. The potential applications include those in high load bearing environments, including mechanical, transportation, industrial and other fields, to save energy and reduce CO_2 emissions. Furthermore, it is an excellent example to determine the relationship between structure and properties.

Conflicts of interest

There are no conflicts to declare.

Acknowledgements

References

1 X. Zhang, G. Liao, Q. Jin, X. Feng and X. Jian, *Tribol. Int.*, 2008, **41**, 195–201.

2 M. Sumer, H. Unal and A. Mimaroglu, *Wear*, 2008, **265**, 1061–1065.

3 Y. Shang, Y. Zhao, Y. Liu, Y. Zhu, Z. Jiang and H. Zhang, *High Perform. Polym.*, 2018, **30**, 153–160.

4 A. M. Díez-Pascual, M. Naffakh, M. A. Gómez, C. Marco, G. Ellis, M. T. Martínez, A. Ansón, J. M. González-Domínguez, Y. Martínez-Rubi and B. Simard, *Carbon*, 2009, **47**, 3079–3090.

5 Z. Zhang, C. Breidt, L. Chang, F. Haupert and K. Friedrich, *Composites, Part A*, 2004, **35**, 1385–1392.

6 Z. P. Lu and K. Friedrich, *Wear*, 1995, **181–183**, 624–631.

7 D. S. Bangarusampath, H. Ruckdäschel, V. Altstädt, J. K. W. Sandler, D. Garray and M. S. P. Shaffer, *Polymer*, 2009, **50**, 5803–5811.

8 H. Unal and A. Mimaroglu, *J. Reinf. Plast. Compos.*, 2006, **25**, 1659–1667.

9 Q.-J. X. Qi-Hua Wang, W.-M. Liu and J.-M. Chen, *Wear*, 2000, **243**, 140–146.

10 J. N. Panda, J. Bijwe and R. K. Pandey, *Composites, Part B*, 2019, **174**, 106951–106969.

11 V. Rodriguez, J. Sukumaran, A. K. Schlarb and P. D. Baets, *Tribol. Int.*, 2016, **103**, 45–57.

12 R. Gilardi, *Lubricants*, 2016, **4**, 20.

13 J. N. Panda, J. Bijwe and R. K. Pandey, *Compos. Sci. Technol.*, 2017, **144**, 139–150.

14 J. Bijwe, K. Kumar, J. N. Panda, T. Parida and P. Trivedi, *Composites, Part B*, 2016, **94**, 399–410.

15 J. N. Panda, J. Bijwe and R. K. Pandey, *Composites, Part A*, 2019, **116**, 158–168.

16 W. Boo, L. Sun, J. Liu, A. Clearfield, H. Sue, M. Mullins and H. Pham, *Compos. Sci. Technol.*, 2007, **67**, 262–269.

17 S. J. Talley, X. Yuan and R. B. Moore, *ACS Macro Lett.*, 2017, **6**, 262–266.

18 Q. Wu, *Chin. Polym. Bull.*, 2013, **26**, 1–6.